

# (26) EXPERIMENTAL AND ANALYTICAL STUDIES ON SEISMIC BEHAVIOR OF EWECs COLUMNS WITH SHEAR STUDS

FAUZAN<sup>1</sup> Hiroshi KURAMOTO<sup>2</sup> and Tomoya MATSUI<sup>3</sup>

<sup>1</sup>Post Doctoral Researcher, Dept. of Civil & Arch. Eng., Toyohashi Univ. of Technology  
(1-1 Hibarigaoka, Tempaku cho, Toyohashi, Aichi 441-8580, Japan)  
E-mail: f049101@edu.imc.tut.ac.jp

<sup>2</sup>Member of JSCE, Associate Professor, Dept. of Civil & Arch. Eng., Toyohashi Univ. of Technology  
(1-1 Hibarigaoka, Tempaku cho, Toyohashi, Aichi 441-8580, Japan)  
E-mail:kura@tutrp.tut.ac.jp

<sup>3</sup>Assistance Professor, Inst., Dept. of Civil & Arch. Eng., Toyohashi Univ. of Technology  
(1-1 Hibarigaoka, Tempaku cho, Toyohashi, Aichi 441-8580, Japan)  
E-mail:matsui@tutrp.tut.ac.jp

This paper presents the results of experimental and analytical studies on the seismic behavior of Engineering Wood Encased Concrete-Steel (EWECs) composite columns. Two column specimens were tested under constant axial load and lateral load reversals that simulated seismic loading. The main test variable was the presence of shear studs. The test results indicated that EWECs columns had excellent hysteretic behavior without severe damage, even at large story drift of 0.04 radian. The results also showed that the presence of shear studs on EWECs columns improved the ductility of the column and reduced the damage of woody shell. Furthermore, an analytical study was conducted using fiber section analysis to simulate the behavior of the columns which is compared with the experimental data.

*Key Words* : column, composite structure, woody shell, shear stud, seismic test, fiber section analysis

## 1. INTRODUCTION

A new type of composite columns called “Engineering Wood Encased Concrete-Steel” (EWECs) composite columns is being developed in new hybrid structural system. The proposed composite column consists of concrete encased steel (CES) core with an exterior woody shell, as shown in **Figs. 1(c)** and **(d)**.

Both economical and structural benefits are realized from this type of composite column due to the use of woody shell as column cover. During construction, the woody shell acts as forming for the composite column, decreasing the labor and materials required for construction and, consequently, reducing the construction cost and time. From the structural point of view, the shell improves the structural behavior of the column

through its action to provide core confinement and resistance to bending moment, shear force and column buckling. These advantages make EWECs columns possible as an alternative to SRC columns, which have weaknesses due to difficulty in constructing both steel and reinforced concrete (RC)<sup>1)2)</sup>.

In our previous study<sup>3)4)</sup>, the structural behavior of an EWECs column using double H-section steel (**Fig. 1c**) had been investigated to apply to columns subjected to bending moments and shear forces in two directions, such as those in the frame structures. It was found that the EWECs column had a stable spindle-shaped hysteresis characteristic without degradation of load-carrying capacity until the maximum story drift angle,  $R$  of 0.05 radian. Furthermore, EWECs columns using single H-section steel, shown in **Fig. 1(d)**, are being

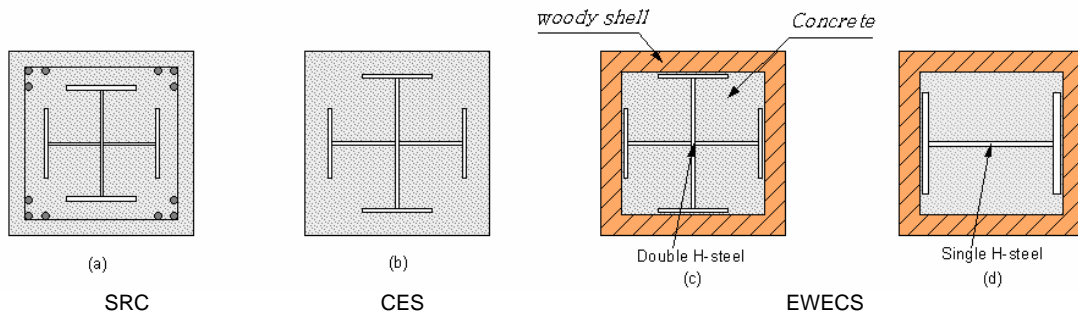


Fig. 1 Types of composite columns

developed to apply to columns in one-way moment frame connected with shear wall in the orthogonal directions.

This paper presents the results of a feasibility study on the structural behavior of EW ECS composite columns using single H-section steel subjected to combined constant axial load and lateral load reversals that simulated earthquake loading. The presence of shear studs was selected as the main experimental parameter in this study in order to investigate the effects of the shear studs to the seismic behavior of the EW ECS columns. An analytical study was also conducted using fiber section analysis in order to compare with the experimental data.

## 2. EXPERIMENTAL PROGRAM

### (1) Specimens and materials used

Two composite column specimens, WSA and WSB, of which the scale is about two-fifth, were tested. The dimensions and details of the specimens are shown in Fig. 2 and Table 1. The main difference between the two specimens was the presence of shear studs using steel bolts, attached from the woody shell to CES core along the column height, as shown in Fig. 3. The purpose of the shear studs is to enhance the bond between the CES core and the woody shell, thereby increasing the composite action of the column.

Both specimens had a column with 1,600 mm height and 400 mm square section. The thickness of the woody shell was 45 mm and the steel encased in each column had a single H-section steel of 300x220x10x15 mm. The mechanical properties of the steel and the woody shell are listed in Tables 2 and 3, respectively. Normal concrete of 35 and 27 MPa was used for Specimens WSA and WSB, respectively. The mix proportions and mechanical properties of the concrete are given in Table 4.

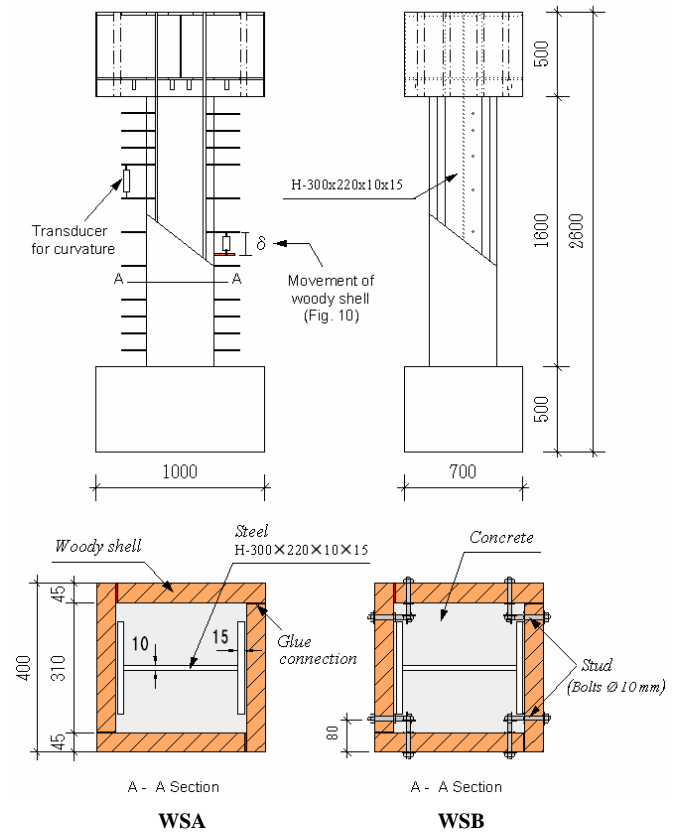


Fig. 2 Test specimen

Table 1 Test program

Specimen	WSA	WSB
Woody shell - core connection	-----	With studs
Woody Shell Thickness (mm)	45	
Concrete strength (MPa)	35	27
Built-in steel (mm)	H-300 x 220 x 10 x 15	
Column Height: h (mm)	1600	
Cross section : b x D (mm)	400 x 400	
Axial Compression	N (kN)	1031
	N/N <sub>tot</sub>	0.16    0.18
Calculated Ultimate flexural strength: Q <sub>mcal</sub> (kN)	712.3	703.2

N<sub>tot</sub> : Total compressive strength of column

**Table 2** Mechanical properties of steel

Steel	Yield Stress $\sigma_y$ (Mpa)	Max. Stress $\sigma_s$ (MPa)	Notes
H-300x	284	450.5	Flange
220x10x15	295.5	454.9	Web

**Table 3** Mechanical properties of woody shell

Woody Shell panel (mm)	Wood type	*Comp. Strength $\sigma_w$ (MPa)	Elastic Modulus $E_s$ (GPa)
40x160x4.5	Glue laminated pine wood	45	11.5

\* the direction is parallel to axis of grain

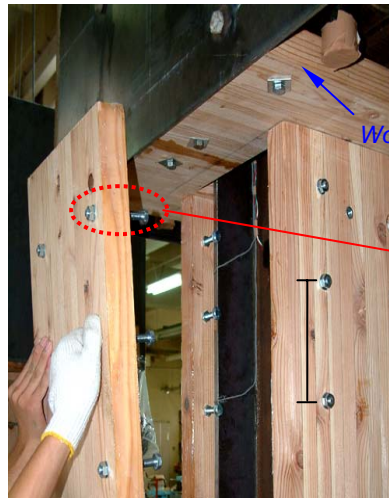
**Table 4** Mix proportions and mechanical properties of concrete

Specimen	W/C (%)	S/(S+G) (%)	Slump (cm)	Unit weight (kg/m <sup>3</sup> )					Comp. Strength MPa
				Water (W)	Cement (C)	Sand (S)	Gravel (G)	Admixture (A)	
WSA	52	46.8	18	182	350	1060	816	3.5	35
WSB	57	48	17	181	318	856	989	3.18	27



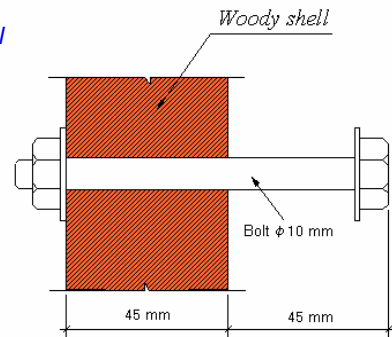
Studded woody panel

(a)



Assembling of studded woody panels to column

(b)



Detail of stud

(c)

**Fig. 3** Fabrication of specimen WSB

In manufacturing the specimens, the steel sections were accurately cut to size of the column and stub first. Then the woody shell panels were assembled to the column by using epoxy. For Specimen WSB, the studs were installed to the woody panels before assembling the panels to the column (**Fig 3**). Finally, the concrete was cast into the column without additional formwork because the woody shell serves as mold forms for concrete placement.

The ultimate flexural strengths for each column shown in **Table 1** were calculated by flexural analysis in which the modified Kent and Park model<sup>5</sup> and the perfect elasto-plastic model were used for the stress-strain relationships of confined concrete and steel, respectively. On the other hand, the original Kent and Park model<sup>6</sup> was used for stress-strain relationship of woody shell in which the mechanical properties of the woody shell except the young modulus ( $E$ ) and the compressive strength were assumed to be the same as those of concrete.

## (2) Test setup and loading procedures

The specimens were loaded lateral cyclic shear forces by a horizontal hydraulic jack and a constant axial compression of 1031 kN by two vertical hydraulics jacks, as shown in **Fig. 4**. Considering the cross section of the woody shell, the applied axial force ratio,  $N/N_{tot}$ , for Specimens WSA and WSB were 0.16 and 0.18, respectively (see **Table 1**).

The loads were applied through a steel frame attached to the top of a column that was fixed to the base. The incremental loading cycles were controlled by story drift angles,  $R$ , defined as the ratio of lateral displacements to the column height,  $\delta/h$ . The lateral load sequence consisted of two cycles to each story drift angle,  $R$  of 0.005, 0.01, 0.015, 0.02, 0.03 and 0.04 radians followed by half cycle to  $R$  of 0.05 rad. For Specimen WSB, the test was continued until story drift,  $R$  of 0.067 rad., as shown in **Fig. 5**, because the specimen was still capable to resist the applied force after  $R$  of 0.05 rad.

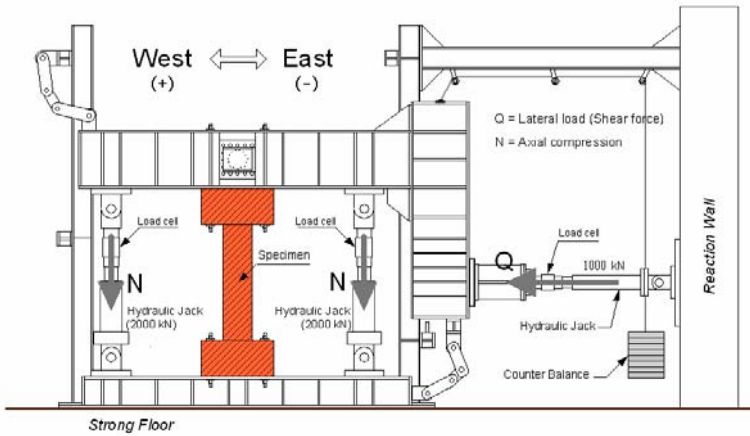


Fig. 4 Schematic view of test setup

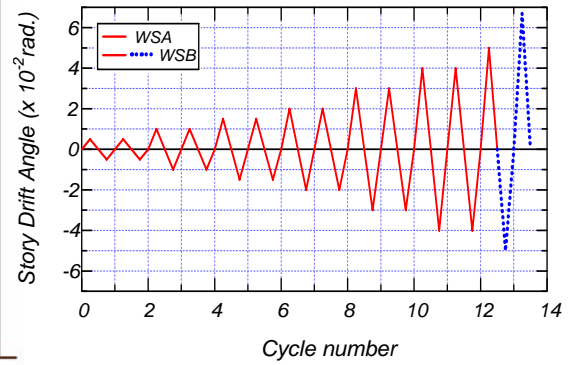


Fig. 5 Loading history

### 3. EXPERIMENTAL RESULTS AND DISCUSSIONS

#### (1) Hysteresis characteristics and failure modes

Shear versus story drift angle relationships of both specimens are given in Fig. 6. In this figure, the predicted flexural capacities calculated by flexural analysis are shown by dashed-dotted lines. The yield and maximum strengths and the corresponding story drift angles for each specimen are listed in Table 5. The yielding of each specimen was assumed when the first yielding of steel flange at the top and bottom of the columns was observed, which corresponds to a triangle mark on the shear versus story drift angle response (see Fig. 6). Crack modes on column faces of both specimens at R of 0.05 and 0.067 rad. are presented in Fig. 7.

From Fig. 6, it can be seen that both specimens showed ductile and stable spindle-shaped hysteresis loops without degradation of load-carrying capacity until large story drift, R of 0.05 and 0.067 radians for Specimens WSA and WSB, respectively. The measured maximum flexural strengths fairly agreed with the calculated strengths.

In Specimen WSA, column without shear studs, the first cracks on the woody shell first appeared at around 30 cm away from the top of the column face at story drift, R of 0.03 rad. Subsequently, the cracks extended along the column height with an increase of the story drift angle. The first yielding of steel flange occurred at R of 0.005 rad. and a shear force of 386 kN. Although the cracks propagated, the shear force slightly increased until maximum capacity of 706.5 kN was reached at R of 0.05 rad. In addition, uplift of woody shell at the column-stub connection was observed significantly after R of 0.03 rad.

Compared with Specimen WSA, Specimen WSB with shear studs resulted in an increase ductility. Up

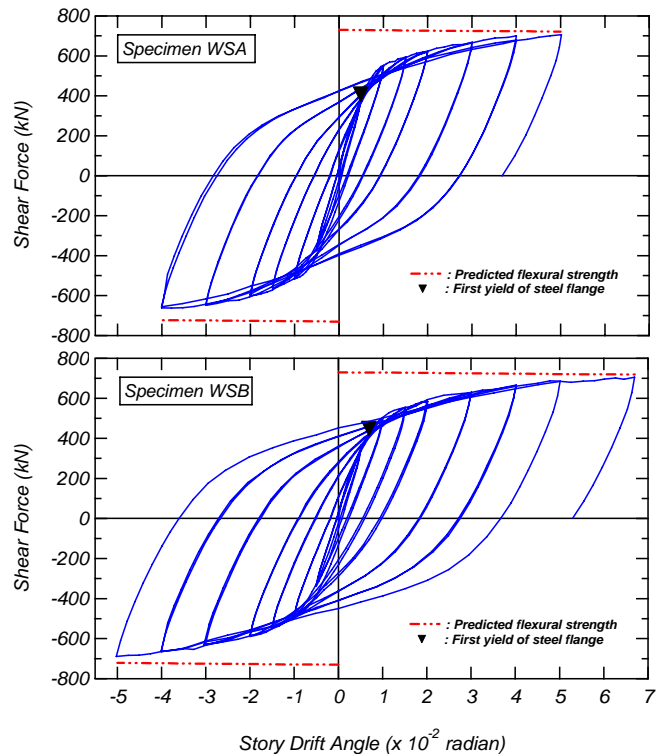


Fig. 6 Shear force - story drift angle relationships

Table 5 Measured strength

Specimen	at Yielding		at the Max. Capacity	
	Q <sub>y</sub> (kN)	R <sub>y</sub> (rad.)	Q <sub>max</sub> (kN)	R <sub>max</sub> (rad.)
WSA	386	0.005	706.5	0.05
WSB	427.6	0.007	705.2	0.067

to a story drift, R of 0.04 rad., no damage was observed on the column faces. Then a little crack occurred at column faces at R of 0.05 rad. For this reason, the test of this specimen was continued until R of 0.067 rad. Although the higher displacement was applied to this specimen, the damage of the column was less than that of Specimen WSA (Fig. 7) due to the enhancement of bond between woody shell and CES core by the shear studs. Also, the

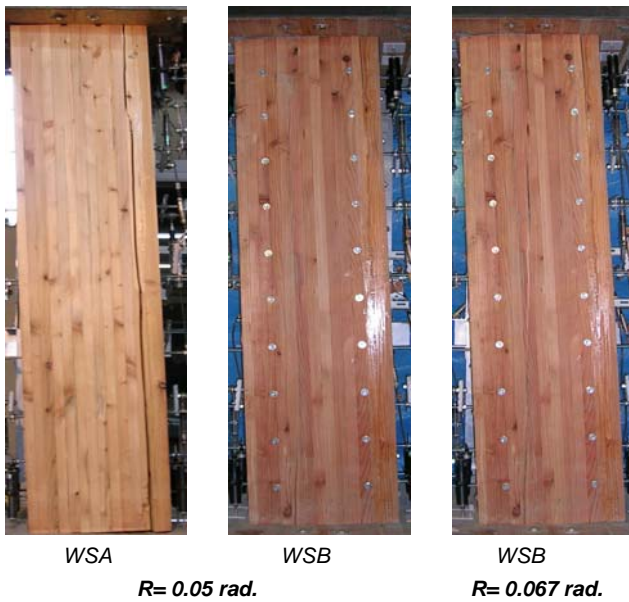


Fig. 7 Crack modes at R of 0.05 and 0.067 radians

brittle failure of this specimen was not significant during testing. The first yielding of steel flange occurred at R of 0.007 rad. and a shear force of 427.6 kN, and the maximum strength of 705.2 kN was reached at R of 0.067 rad.

Figure 8 shows the comparison of sink and uplift displacements of the woody shell at the column-stub joint at each story drift angle for both specimens. The values were obtained by measuring the vertical displacement between woody shell and wood panel at the joint using transducers. It can be seen from these figures that both specimens had almost the same value of sink displacement until R of 0.04 rad. However, the uplift of Specimen WSB was smaller than that of Specimen WSA due to the presence of the shear studs.

Figure 9 compares the movement of the woody shell from the CES core until R of 0.03 rad. for both specimens. The values were obtained by measuring the displacement between the CES core and the woody shell using vertical transducers installed at the encased steel and the woody shell at the top, middle and bottom of the column, as shown in Fig. 2. From Fig. 9, it can be seen that the movement of the woody shell from the CES core at the top and middle of the columns was relatively small for both specimens, which is less than 1 mm. Compared with Specimen WSA, Specimen WSB had the smaller movement of the woody shell due to the enhancement of bond between the CES core and the woody shell by the shear studs.

By comparing the hysteresis loops and damage situations of these specimens, it was revealed that both specimens had excellent hysteretic behavior with almost the same maximum capacity. However, Specimen WSB had the higher ductility and better

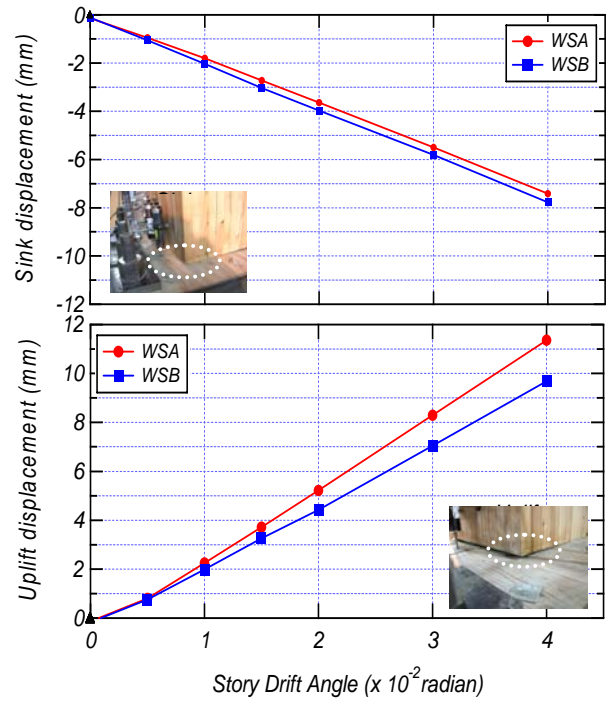


Fig. 8 Sink and uplift displacements of woody shell at column-stub joint

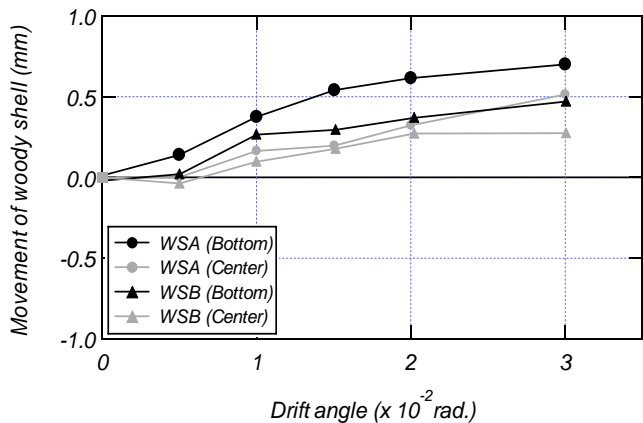
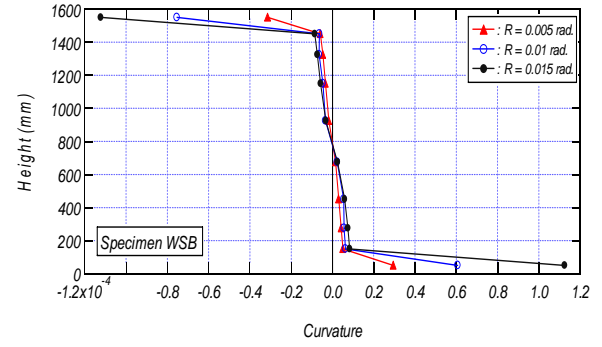
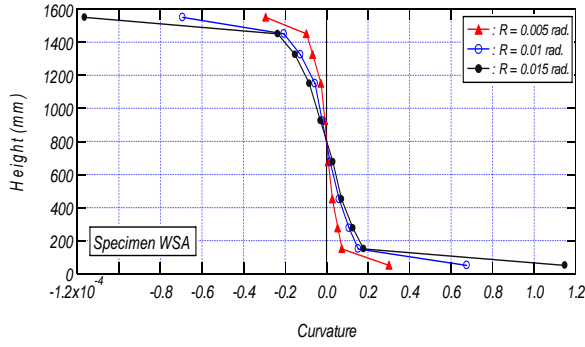


Fig. 9 Movement of woody shell from CES core

performance in propagation of cracks in the woody shell than Specimen WSA. In addition, the presence of shear studs reduced the uplift displacement and movement of the woody shell from CES core. This means that the shear studs improve the structural behavior of EWECs columns by improving composite action of the columns. It was also observed from this study that the woody shell contributed to flexural strength until large story drift, R of 0.067 rad. for Specimens WSB (with shear studs), although the cracks appeared along the column faces after R of 0.04 rad. (see Figs. 6 and 7).

## (2) Curvature distribution

Figure 10 shows the curvature distributions along the column height at R of 0.005, 0.01 and 0.015 radians for both specimens. The values were obtained from transducers installed on the two



**Fig. 10** Curvature distribution

opposite sides along the column height, as shown in **Fig. 2**. As seen in **Fig. 10**, the distribution of curvature was almost identical at each story drift angle for both specimens in which the highest curvature occurred at both the top and bottom of the column. However, the curvature distribution slopes of Specimen WSB were smaller than that of Specimen WSA due to the increase of composite action by the shear studs.

#### 4. ANALYTICAL INVESTIGATIONS

##### (1) Summary of analytical study

Fiber section analysis method was used to construct moment-curvature relationships of critical section. In the method, the cross section is discretized into a number of small areas or filaments, as shown in **Fig. 11**. Each fiber is assumed to be uniaxially stressed and to behave according to assumed hysteresis stress-strain characteristic of its constituting materials, as explained below. In this study, the cross section of column was divided into 40 elements. This method assumes that the plane sections to remain plane, thus implying full compatibility between the steel, concrete and woody shell components of a composite cross section.

The analysis is controlled through a series of small steps by curvature or displacement history in terms of X-axis. With the axial strain at the center of

the cross section,  $\Delta\varepsilon_0$  and the curvatures along in terms of X-axis,  $\Delta\phi_x$ , the axial strain at the fiber element of  $i$ ,  $\Delta\varepsilon_i$  is found according to

$$\Delta\varepsilon_i = \Delta\varepsilon_0 + y_i \Delta\phi_x \quad (1)$$

where  $y_i$  is the distance from the X-axis to the  $i$ th fiber element on the section.

Considering the equilibrium of the section, axial force  $\Delta N$  and bending moment  $\Delta M$  are written as follows, using stiffness matrix  $[K]$ ;

$$\{\Delta N, \Delta M\}^T = [K] \{\Delta\varepsilon_0, \Delta\phi_x\}^T \quad (2)$$

In this analysis,  $\Delta N$ ,  $\Delta M$  and  $\Delta\varepsilon_0$  were calculated by satisfying Eqs. (1) and (2), and considering the mechanical properties of steel, concrete and woody shell, as  $\Delta\phi_x$  was the input data. Load-displacement relations for the columns were obtained assuming an antisymmetric distribution of bending moments along the column height, with the inflection point at midheight. Considering the experimental results for curvature distribution along the column height (**Fig. 10**), the relation between curvature and displacement rotation angles,  $R$  was assumed as  $\phi = 2.2 R/L$ , although in elastic assumption the relation is defined as  $\phi = 6 R/L$ , where  $L$  is the column height.

The hysteretic model used for the steel frame was the trilinear model proposed by Shibata<sup>7)</sup>, as shown in **Fig. 12**. Yield strengths in both compression and

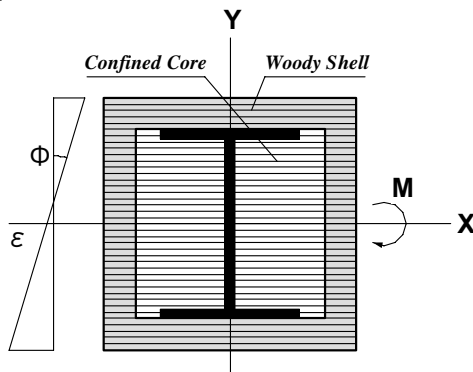


**Fig. 11** Fiber model

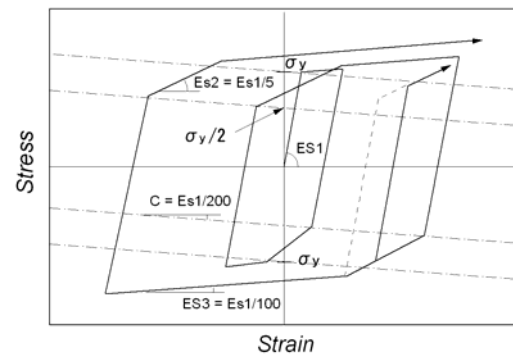


**Fig. 12** Stress-strain model of steel

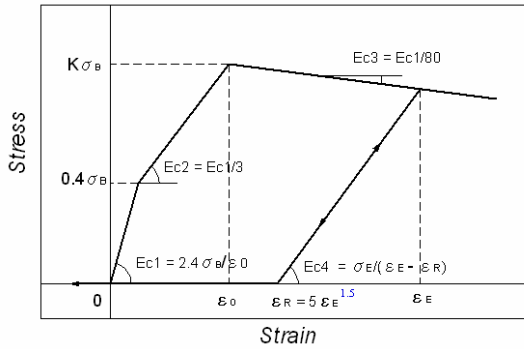


Fig. 13 Stress-strain model of confined concrete

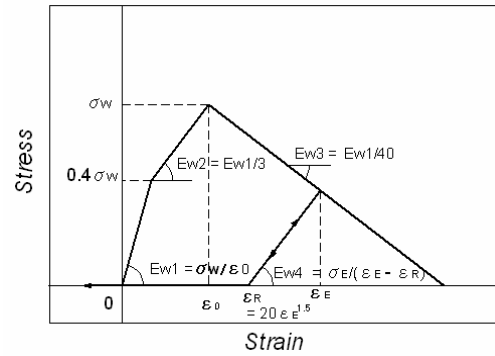


Fig. 14 Stress-strain model of woody shell

tension were assumed to be equal.

The hysteretic model of confined concrete adopted was the divided linear model<sup>8)</sup>, as shown in Fig. 13. In this model, a magnification factor of concrete strength  $K$  for confined core concrete was considered as 1.15 and the compressive strain at the stress peak,  $\varepsilon_0$  was taken as 0.0036.

The hysteretic model of woody shell used was almost similar to the concrete model that is divided linear model, as shown in Fig. 14. The compressive strain at the stress peak,  $\varepsilon_0$  was taken as 0.004.

## (2) Analytical results

According to the assumption of this analysis about the full compatibility between the steel, concrete and woody shell components of a composite cross section, the fiber section analysis results were compared to the experimental data of EWECs column with shear studs (Specimen WSB), as shown in Fig. 15. From this figure, it can be seen that the analytical results for shear force-story drift relationships of the specimen showed a good agreement with the test results. The analytical models adequately simulated the behavior of the test

specimen. These comparative good results confirmed the accuracy of the proposed numerical analysis to predict the ultimate flexural strength and behavior of EWECs columns under constant axial load and lateral load reversals.

Figure 16 shows the contributions of steel, concrete and woody shell to shear force with an increase of story drift angle. As seen in this figure, the steel gave much contribution to shear force, while the contribution of woody shell was slightly higher than that of concrete. The contribution of concrete to shear force increased until  $R$  of 0.03 rad., on the other hand, the contribution of woody shell tended to be constant after  $R$  of 0.04 rad. This result indicated that the crack of woody shell occurred after  $R$  of 0.04 rad., which was in good agreement with the visual observation during testing. From this figure, it can also be seen that the woody shell contributed to shear force until the maximum story drift,  $R$  of 0.067 rad., which fully agreed with the experimental data.

The contributions of steel, concrete and woody shell to axial load at each story drift angle are presented in Fig. 17. It is revealed from this figure that the concrete and woody shell contributed mostly

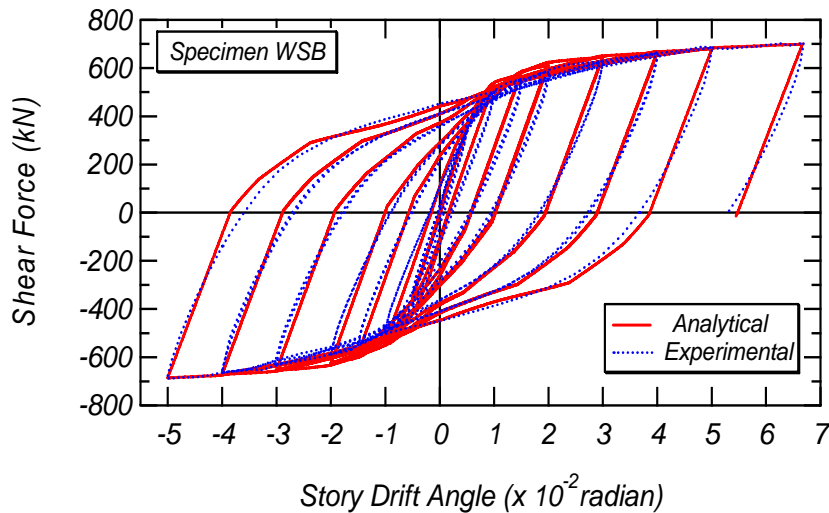


Fig. 15 The comparative results of shear force-story drift angle relationships

to resist axial compression, while the steel contributed to the tension. In addition, this figure also confirms the experimental data that the woody shell contributed to resist the axial compression until maximum story drift,  $R$  of 0.067 rad.

## 5. CONCLUSIONS

Based on the studies presented here, the following conclusions can be drawn:

1. EW ECS columns using single H-section steel had excellent structural performance without severe damage, even at large story drift angle,  $R$  of 0.04 rad.
2. The presence of shear studs on EW ECS columns improved the ductility of the column and reduced the damage of woody shell.
3. With shear studs, the woody shell contributed to flexural capacity until large story drift angle,  $R$  of 0.067 rad., although cracks appeared at the column faces after  $R$  of 0.04 rad.
4. The calculated hysteresis loops using fiber analysis showed a good agreement with the experimental results. This indicates that the analytical method can be used to predict accurately the ultimate strength and behavior of EW ECS columns.
5. The analytical results confirmed the test data for the contributions of woody shell to shear force and axial load until  $R$  of 0.067 rad.

## REFERENCES

- 1) Kuramoto H., Takahashi H. and Maeda M. Feasibility Study on Structural Performance of Concrete Encased Steel Columns using High Performance Fiber Reinforced Cementitious Composites. *Summaries of Technical Papers of Annual Meeting, AIJ*, Vol.C-1, 2001.
- 2) Kuramoto H., Adachi T. and Kawasaki K. Behavior of Concrete Encased Steel Composite Columns Using FRC. Proceedings of Workshop on Smart Structural Systems Organized for US-Japan Cooperative Research Programs on Smart Structural Systems (Auto-Adaptive Media) and Urban Earthquake Disaster Mitigation, Tsukuba-Japan, 2002.
- 3) Fauzan, Kuramoto H., Shibayama Y. and Yamamoto T. Structural Behavior of Engineering Wood Encased Concrete-Steel Composite Columns. *Proceedings of the Japan Concrete Institute (JCI)*, Vol. 26, No.2, 2004.
- 4) Kuramoto H and Fauzan. Feasibility Study on Engineering Wood Encased Concrete-Steel Composite Columns. *Proceedings of 11<sup>th</sup> ICSGE*, CD-ROM, 2005.
- 5) Park R., Priestley M.J.N. and Gill W.D. Ductility of Square-Confined Concrete Column. *Proceedings of ASCE*, Vol. 108, No. ST4, pp. 929-950, 1982.
- 6) Kent D.C. and Park R. Flexural Members with Confined Concrete. *Proceedings of ASCE*, Vol. 97, No. ST7, pp. 1969-1990, 1971.
- 7) Shibata M. Analysis of Elastic-Plastic Behavior of Steel

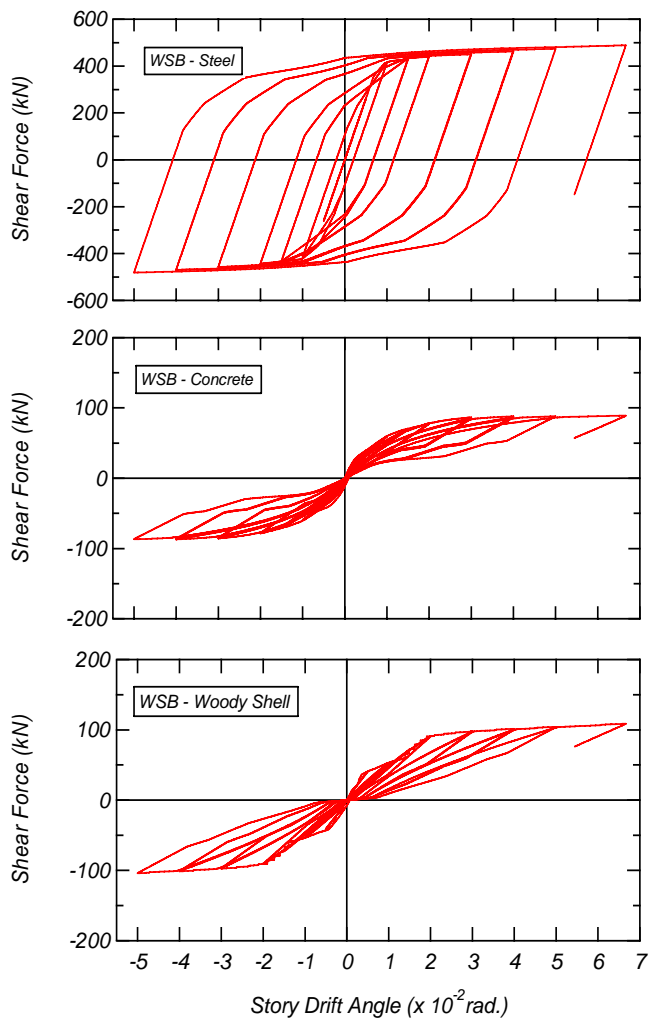


**Fig. 16** Contributions of steel, concrete and woody shell to shear force

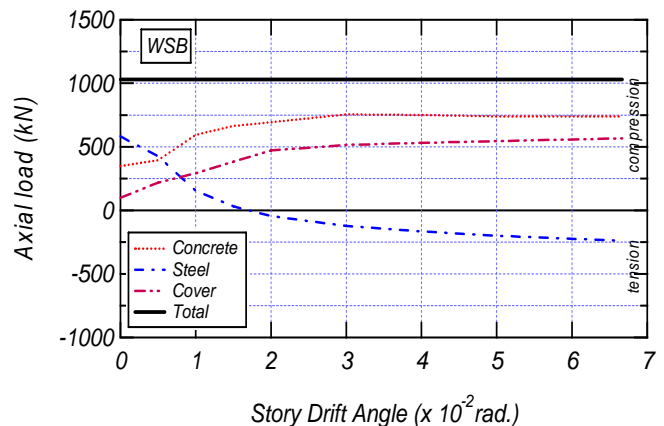


**Fig. 17** Contributions of steel, concrete and woody shell to resist axial load

Brace Subjected to Repeated Axial force. *International Journal of Solids and Structures*, Vol. 8, No. 3, pp. 217-228, 1982.

- 8) Kuramoto H., Kabeyasawa T. and Shen F-H. Influence of axial deformation on ductility of high-strength reinforced concrete columns under varying triaxial forces. *ACI Structural Journal*, Vol. 92, No. 5, pp. 610-618, 1995.